

## AN ECONOMICAL SEMI-ANALYTICAL ORBIT THEORY FOR RETARDED SATELLITE MOTION ABOUT AN OBLATE PLANET

Robert A. Gordon  
Goddard Space Flight Center

### ABSTRACT

Brouwer and Brouwer-Lyddanes' use of the Von Zeipel-Delaunay method is employed to develop an efficient analytical orbit theory suitable for micro-computers. A succinctly simple pseudo-phenomenologically conceptualized algorithm is introduced which accurately and economically synthesizes modeling of Drag effects. The method epitomizes and manifests effortless efficient computer mechanization. Simulated (Space Telescope) trajectory data is employed to illustrate the theory's ability to accurately accommodate oblateness and Drag effects for micro-computer ground based or on-board predicted orbital representation. Real (SMM – Solar Maximum Mission) tracking data is used to demonstrate that the theory's orbit determination and orbit prediction capabilities are favorably adaptable to and are comparable with results obtained utilizing complex "Definitive Cowell Method" solutions on satellites experiencing significant Drag effects.

AN ECONOMICAL SEMI-ANALYTICAL ORBIT THEORY FOR  
RETARDED SATELLITE MOTION ABOUT AN OBLATE PLANET

BY: ROBERT A. GORDON  
(NASA/GSFC)

INTRODUCTION:

Brouwer<sup>1</sup> derived a first-order perturbation solution expressing the secular, short and long periodic variations in the motion of an artificial satellite about an oblate planet. Brouwer obtained separation of all the periodic terms by adapting Von Zeipel's<sup>2</sup> technique to modify Delaunay's method for calculating the coefficients of the periodic terms through a succession of canonical transformations. Delaunay's variables were introduced in order to simplify the canonical expressions for the equations of motion. Brouwer developed the periodic terms to  $O(J_2)$  and obtained the secular variations to  $O(J_2^3)$ . The resultant formulas are piecewise continuous with singularities existing for certain values of the eccentricity and inclination which occur as poles in the algebraic expressions. Thus, the equations are valid, except in the regions for which  $e''=0$ ,  $i''=0$  deg. , and  $1-5\cos^2 i'' = 0^\circ$  i.e.,  $i''=63.43^\circ$ , the critical inclination. Lyddane<sup>3</sup> introduced Poincaré's variables and reformulated Brouwer's expressions as to remove the poles, and thus the singularities arising from small eccentricities or inclinations in the Brouwer theory.

This paper is the fruition of an effort to provide an optimal on-board ephemeris representation employing an efficient analytical orbit theory suitable for micro-computers. Brouwer/Brouwer-Lyddane's method is modified to develop an economical

analytical orbit theory for satellite motion about an oblate planet which accommodates  $J_2$ ,  $J_3$ , and parts of the  $J_4$  zonal effects with the true argument of latitude as the fast variable. The theory is applicable to circular and non-circular satellites but singular for  $i=0$ . This is satisfactory for the vast majority of our satellite support. The choice of the true argument of latitude as the fast variable in difference to Brouwer-Lyddane's choice of the true longitude is a major contribution to the economical variation presented here; it simplifies the computation of the osculating inclination.  $J_3$  and portions of the  $J_4$  zonal effects are considered in the theory in relation to their primary effects on the radial and cross-track errors respectively, and truncated in accordance with economical computational consideration. Lyddane remarks that  $l''$  and  $g''$  must be used for computing  $f'$  and  $r'$  in his version; however, as demonstrated by Gordon<sup>4</sup> et al., this results in a relative large radial error with respect to Brouwer for moderate values of the eccentricity. This can be avoided by evaluating  $f'$  and  $r'$  with  $l', g'$  for moderate values of the eccentricity and with  $l'', g''$  for relative low values of the eccentricity. The theory presented here also computes  $f'$  and  $r'$  with the long-period contribution ( $J_3$ ) to the eccentricity. For some orbital parameters, this can result in a significant improvement in accounting for intrack error due to the oblateness perturbation and compares favorably with respect to the Brouwer and Brouwer-Lyddane's orbit theories for the satellite cases presented in Reference 4. The theory presented here is further modified to incorporate a "cheap" algorithm which accounts for drag effects semi-analytically. A succinctly simple pseudo-phenomenologically conceptualized algorithm is introduced which accurately and economically synthesizes modeling of drag effects. The method epitomizes and manifests effortless efficient computer mechanization. Simulated (Space Telescope) trajectory data is employed to illustrate the theory's ability to accurately accommodate oblateness and drag effects for microcomputer ground-based or on-board

predicted orbital representation. Real (SMM-Solar Maximum Mission) tracking data is used to demonstrate that the theory's orbit determination and orbit prediction capabilities are favorably adaptable to and comparable with results obtained utilizing complex "Definitive Cowell Method" solutions on satellites experiencing significant drag effects.

FORMULAS FOR COMPUTATION:

A computational flow diagram of a subroutine with a description of input and output parameters for that part of the modified Brouwer theory which accounts for the oblateness effects is presented in the Appendix. Henceforth, this analytic part of the current orbit theory will be represented by the symbolic function  $Bg(t)$ , where  $t$  designates the time of theory evaluation.

The theory is adapted to accommodate retarded motion due to drag by a pseudo-physical secular relationship to describe decay in the semi-major axis. This representation is inferred phenomenologically from the signature of the semi-major axis Locus defined by osculating to mean<sup>5</sup> conversions of state vectors of a drag perturbed satellite ephemeris.

OSCULATING-TO-MEAN CONVERSION:

Walter's algorithm<sup>5</sup> for osculating to mean conversion is unstable for low  $e$  in Keplerian space; the apparent instability of the iterative osculating-to-mean element conversion is removed by translating the iteration from mean Keplerian space to mean Cartesian space.

Define:

$$\begin{aligned} \bar{\Omega} &\equiv (a^*, e^*, i^*, g^*, h^*, l^*) \text{ -- Mean Keplerian Elements} \\ \Omega &\equiv (a, e, i, g, h, l) \text{ -- Osculating Keplerian Elements} \end{aligned}$$

$X \equiv (x'', y'', z'', \dot{x}'', \dot{y}'', \dot{z}'')$  -- Mean Cartesian State Elements

$Y \equiv (x, y, z, \dot{x}, \dot{y}, \dot{z})$  -- Osculating Cartesian State Elements

Given an osculating Cartesian state  $Y$  we determine

$$\bar{\Omega}_i^{(0)} \leftarrow f_{2B}(Y_i)$$

Where  $f_{2B}$  represents the Keplerian state two-body functional relationship to the Cartesian state. Then employing the iterative algorithm,

$$\begin{aligned} \bar{\Omega}^{(j)} &\leftarrow B_9(\Delta t=0, \bar{\Omega}^{(j)}) \\ Y^{(j)} &\leftarrow f_{2B}(\bar{\Omega}^{(j)}) \\ X_i^{(j+1)} &= X_i^{(j)} + (Y_i - Y_i^{(j)}), \quad i = 1, 2, \dots, 6 \\ \bar{\Omega}^{(j+1)} &\leftarrow f_{2B}^{-1}(X^{(j+1)}) \end{aligned}$$

For  $j = 0, 1, 2, \dots, 10$  or until the following criterion is satisfied:

$$|Y_i - Y_i^{(j)}| \leq \epsilon$$

Where  $\epsilon$  is some preassigned small positive number. Let this algorithm be represented by the symbolic functional relationship,

$$\bar{\Omega} \leftarrow O(Y)$$

#### SEMI-MAJOR AXIS DECAY RATE:

Applying the osculating to mean conversions at one period ( $P$ ) intervals, we determine the semi-major axis decay over  $M$  periods, i.e., with

$$a_i'' \leftarrow O_i(\bar{\Omega})$$

Given for  $i = 1, 2, \dots, M$ ; we compute the mean semi-major axis decay rate as

$$\dot{a}_i'' = \sum_{i=1}^M \left( \frac{a_i'' - a_{i-1}''}{M} \right)$$

## ORBIT PROPAGATION WITH "Bg":

To update the orbital elements to time ( $\Delta t = t - t_0$ ) with the  $\dot{B}_g$  theory, we assume the orbital elements remain constant over one period and rectify the theory's constants at one period intervals (with the  $\dot{a}$  decay rate) up to the Nth period where

$$N = \text{int} \left( \frac{\Delta t}{P} \right).$$

Employing the above iterative method we have

$$\begin{aligned} a''_j &= a_{j-1} + \dot{a} P_{j-1} \\ e''_j &= e_{j-1} + \frac{(1 - e_{j-1})}{a_{j-1}} \dot{a} P_{j-1} \end{aligned}$$

$$(l''_0)_j = (l''_0)_{j-1} - \frac{3}{4} \left( \frac{n_{j-1}}{a_{j-1}^3} \right) \dot{a} P_{j-1}^2, \quad n = \sqrt{\frac{\mu}{a^3}}$$

Evaluating the secular part of  $B_g$  we obtain

$$\bar{\Omega}_j \leftarrow B_g''(P_{j-1})$$

Where  $j = 1, 2, \dots, N \Rightarrow$

$$\bar{\Omega}_N \equiv (a''_N, e''_N, i''_N, g''_N, h''_N, l''_N)$$

Then at time  $\Delta t$  the osculating elements are given by evaluating the full  $B_g$  theory with

$$\underline{\Omega}(\Delta t) \leftarrow B_g(\bar{\Omega}(T_N), \Delta t - T_N)$$

With  $T_N = N \times P$ . Let us represent the semi-analytic theory with the rectification algorithm for retarded motion symbolically by " $\dot{B}_g$ ."

## TRAJECTORY DATA:

Trajectory data, i.e., osculating state vectors are used in a simulation to demonstrate the  $\dot{B}_g$  orbit theory capability in representing retarded satellite motion about an oblate planet. It has been proposed that a secular analytic orbit theory be employed for the on-board ephemeris representation of the Space Telescope. The

Space Telescope can experience significant drag effects over a three-day span. State vectors generated from a sample set of Space Telescope elements demonstrates the Bg theory's superior ability to represent the Space Telescope ephemeris. This will be demonstrated by three steps in the simulation.

Step No. 1:

A comparison is made between two Cowell ephemeris generations at two-hour intervals, the "Truth Ephemeris" with drag included with a drag model constant  $C_D = 2.0$  versus the Cowell ephemeris with  $C_D = 0$ , i.e., no drag consideration over a three-day span. The Space Telescope epoch elements is defined as:

$a$	= 6778.140 km	$A$	= 117.6 m <sup>2</sup>
$e$	= 0.001	$m$	= 10134 kg
$i$	= 28.2 degrees		
$h$	= 19.78 degrees	$h_p$	= 393.222 km
$g$	= 0 degree	$h_a$	= 406.778 km
$l$	= 0 degree		

Note: Table No. 1 -- the maximum total error growth realized was (262.88 km).

Step No. 2:

An analytical method without drag model effects is fitted to the "Truth Ephemeris" over a three-day span with the "Truth Ephemeris" state vectors as observation data at two-hour intervals for a Differential Correction of the epoch mean elements of the analytical orbit theory. The analytical theory used is the Brouwer-Lyddane which includes periodic terms.

Note: Table No. 2 -- the post trajectory data DC compare at the two-hour frequency yields a maximum total error of (43.71 km).

### Step No. 3:

Step No. 2 was repeated employing the  $\dot{B}_g$  orbit theory.

Note: Table No. 3 -- the post trajectory data DC compare at the two-hour frequency yields a maximum total error of (1.30 km).

### TRACKING DATA:

Real tracking data demonstrates the  $\dot{B}_g$  orbit theory's favorable orbit determination and prediction capabilities. An orbit determination for a number of different epochs employs real (SMM-Solar Maximum Mission) tracking data over a two-day span to differentially correct the epoch state and drag model parameter for a "Definitive Cowell Method" and the epoch mean elements for the  $\dot{B}_g$  orbit theory. The predicted ephemeris of the "Definitive Cowell Method" and the  $\dot{B}_g$  orbit theory is then compared with a series of state solutions determined over a two-day DC arc at two-day intervals. A table of the comparable response of the Cowell and  $\dot{B}_g$  method is presented in Table 4.

### CONCLUSIONS:

1. The osculating to mean algorithm described herein provides an accurate first-order estimate to the semi-major axis decay rate.
2. Tables 1 and 2 graphically demonstrates that the  $\dot{B}_g$  orbit theory can accurately accommodate significant drag effects on orbital motion and that the  $\dot{a}$  parameter can absorb virtually all of the significant drag effects.
3. Table 4 implies that the  $\dot{B}_g$  theory is competitive with a "Definitive Cowell Method" in a least squares batch filter orbit determination for



satellites experiencing significant drag effects. Thus this can expand the class of satellites which can be operationally supported with a semi-analytic orbit theory.

4. The  $\dot{B}_g$  theory is suited for a ground-based or on-board microcomputer applications, providing an orbital ephemeris generation which does not require a density table or analytic density model.

#### RECOMMENDATIONS:

1. Some adaptation of the  $\dot{B}_g$  theory should be employed for the on-board ephemeris representation of the Space Telescope.
2. Develop the state transition matrix for a truncated secular version of  $\dot{B}_g$  for Karman Filter state estimation applications on microcomputers.
3.  $\dot{B}_g$  be adapted by those various sites who require orbit ephemeris generation but does not have an orbit determination capacity. The mean orbital constants and the  $\dot{a}$  parameter can be determined and distributed by Goddard for satellites of interest as are now the Brouwer Mean Orbital elements. This would lead to a uniform method at each of the various sites who require such elements with a significant improvement in ephemeris representation for satellites experiencing significant drag effects.

DATE OF DATA		POSITION DIFFERENCES (METERS)			POSITION DIFFERENCES DEGREES				POSITION DIFFERENCES (METERS)		POSITION DIFFERENCES (KM.)		POSITION DIFFERENCES (METERS)		POSITION DIFFERENCES (DEG.)
YYMMDD	HMMSS	DA	PPM DE	(10**3) DI	DELH	DELG	DELM	DELTIME	TOTAL ERROR	RADIAL	IN TRACK	ALONG TRACK	CROSS TRACK	TRUE ANOMALLY	
800101	0.	0.00	0.0	0.00	-0.00	-0.00	0.00	-0.0000	0.00	0.00	-0.00	-0.00	0.00	360.00	
800101	20000.	83.59	24.41	-1.53	-2.27	-0.05	0.06	0.0102	240.24	-80.42	0.08	78.15	-212.47	350.43	
800101	40000.	-127.00	-8.17	-0.96	-3.62	-0.94	0.94	0.0927	721.76	-69.67	0.71	711.72	-97.69	1.24	
800101	60000.	17.94	-10.19	-0.11	-3.63	0.57	-0.56	0.1455	1132.85	70.73	1.12	1116.69	177.08	13.49	
800101	80000.	-178.12	33.25	-0.24	-1.98	0.73	-0.71	0.3103	2410.19	-369.06	2.38	2381.77	5.03	339.56	
800101	100000.	-151.31	3.92	-0.25	-1.10	357.70	-357.67	0.6499	4994.55	-172.92	4.99	4991.17	-61.86	1.60	
800101	120000.	-143.57	-62.50	-0.59	0.54	-0.57	0.62	0.7995	6143.41	276.48	6.14	6136.94	54.85	19.13	
800101	140000.	-267.31	30.37	-1.96	0.80	3.47	-3.40	1.0115	7776.03	-375.61	7.76	7764.87	-179.85	344.47	
800101	160000.	-208.34	54.51	-1.34	-3.09	-1.15	1.25	1.5163	11659.37	-565.02	11.64	11643.32	-234.01	1.41	
800101	180000.	-300.10	-18.26	0.49	-3.84	-2.48	2.60	1.9604	15050.25	-134.43	15.05	15049.23	-112.15	7.71	
800101	200000.	-328.03	-16.43	1.80	-2.37	1.17	358.99	2.4166	18554.05	-190.65	18.55	18552.48	147.85	359.38	
800101	220000.	-463.20	10.98	1.76	-0.07	1.43	-1.23	3.0486	23409.93	-489.38	23.40	23404.04	191.29	355.61	
800102	0.	-346.01	9.18	-0.61	-0.56	-1.21	1.45	3.7498	28793.71	-355.66	28.79	28791.50	22.34	357.94	
800102	20000.	-387.82	-30.11	-0.96	-5.09	0.87	-0.58	4.3352	33282.49	-116.42	33.28	33280.88	306.77	9.53	
800102	40000.	-535.87	23.41	-1.00	-6.99	2.68	-2.35	4.9812	38241.07	-543.28	38.24	38237.20	-24.84	346.46	
800102	60000.	-450.74	25.05	-0.78	-4.87	-1.39	1.77	5.8524	44943.41	-477.19	44.94	44940.08	-267.50	359.53	
800102	80000.	-558.16	-59.85	-0.11	-2.89	-0.35	0.78	6.5768	50486.37	41.35	50.49	50486.29	78.00	12.65	
800102	100000.	-505.33	55.42	-1.28	-1.15	4.61	-4.12	7.3302	56277.95	-564.37	56.28	56275.10	-52.92	348.25	
800102	120000.	-582.19	70.86	-1.36	-1.87	-2.18	2.72	8.4557	64931.37	-728.67	64.93	64927.05	-171.64	4.62	
800102	140000.	-621.43	-64.72	-1.83	-3.82	356.46	-355.86	9.3871	72060.31	207.04	72.06	72059.81	169.50	3.15	
800102	160000.	-672.69	-34.59	-1.31	-3.82	4.05	356.62	10.1744	78116.10	22.44	78.12	78115.85	196.97	357.14	
800102	180000.	-646.32	61.29	1.11	-5.38	1.95	-1.21	11.3165	86879.22	-509.12	86.88	86877.73	-12.47	2.72	
800102	200000.	-739.65	13.62	1.48	-3.37	-1.51	2.33	12.6381	97034.61	-166.98	97.03	97034.12	-259.67	354.53	
800102	220000.	-692.36	-25.74	1.37	-2.44	0.91	-0.01	13.8261	106155.76	313.94	106.16	106155.28	46.86	6.65	
800103	0.	-734.94	31.32	-1.29	-5.87	3.78	-2.79	15.0265	115351.96	48.73	115.35	115351.91	-95.41	355.39	
800103	20000.	-935.52	19.92	-1.56	-5.78	-0.64	1.71	16.4412	126243.38	95.53	126.24	126242.99	-296.90	357.94	
800103	40000.	-715.54	-34.64	0.02	-8.97	-1.16	2.32	17.7319	136131.57	914.00	136.13	136128.31	230.72	8.14	
800103	60000.	-1029.21	-3.00	-0.89	-7.32	5.57	-4.32	18.9784	145708.60	606.19	145.71	145707.18	216.61	352.29	
800103	80000.	-868.53	73.62	0.40	-5.34	-0.52	1.86	20.6096	158243.87	505.38	158.24	158242.86	-252.15	5.82	
800103	100000.	-945.72	-78.58	-0.56	-6.83	-3.02	4.46	22.1222	169827.86	1682.91	169.82	169819.52	12.59	357.00	
800103	120000.	-1120.45	-48.86	-1.89	-1.87	6.08	355.45	23.4078	179744.87	1619.19	179.74	179737.56	63.59	355.90	
800103	140000.	-870.93	108.63	-1.23	-8.39	4.08	-2.44	25.1243	192892.69	1114.23	192.89	192889.14	-357.96	8.79	
800103	160000.	-1203.34	-29.79	-1.36	-9.34	-3.35	5.10	26.9431	206860.50	2062.75	206.85	206850.07	-242.30	352.43	
800103	180000.	-1000.10	-55.88	2.04	-7.64	2.47	-0.61	28.5222	219028.26	2918.11	219.01	219008.62	296.97	2.94	
800103	200000.	-1209.92	11.27	1.93	-9.26	7.35	-5.36	30.2842	232502.55	2673.50	232.49	232487.01	281.67	2.13	
800103	220000.	-1187.26	48.39	-0.02	-3.44	0.19	1.92	32.3532	248429.29	3026.44	248.41	248410.78	-190.99	356.58	
800104	0.	-1008.66	-31.85	0.08	-11.63	-0.11	2.34	34.2400	262918.02	4321.32	262.88	262882.30	329.56	2.74	

Table No. 1 -- Cowell Drag Versus Cowell No Drag

DATE OF DATA		POSITION DIFFERENCES (METERS)			POSITION DIFFERENCES DEGREES				POSITION DIFFERENCES (METERS)			POSITION DIFFERENCES (KM.)			POSITION DIFFERENCES (METERS) (DEG.)	
YYMMDD	HHMMSS	DA	PPM DE	(10**3) DI	DELH	DELG	DELM	DELTIME	TOTAL ERROR	RADIAL	IN TRACK	ALONG TRACK	CROSS TRACK	TRUE ANOMALLY		
800101	0.	594.11	44.91	0.34	1.32	-0.79	1.15	5.6939	43709.82	428.87	43.71	43707.65	-75.40	360.00		
800101	20000.	691.75	-13.88	-1.07	-1.54	-1.96	2.27	4.7809	36712.55	842.27	36.70	36702.59	-147.85	350.43		
800101	40000.	447.19	-36.69	-0.76	-2.31	1.36	-1.11	3.7730	28981.16	752.25	28.97	28971.34	-52.64	1.24		
800101	60000.	624.41	35.66	0.33	-2.13	2.26	-2.06	2.9374	22550.98	373.43	22.55	22547.76	76.82	13.49		
800101	80000.	410.42	9.69	0.07	-0.53	-2.85	3.00	2.2598	17349.19	277.66	17.35	17346.96	16.03	339.56		
800101	100000.	441.00	-42.49	0.09	0.75	-1.42	1.51	1.5277	11755.50	742.22	11.73	11731.97	42.31	1.60		
800101	120000.	449.28	-45.24	-0.25	2.52	3.19	-3.14	0.6968	5387.36	647.62	5.35	5348.24	-21.96	19.13		
800101	140000.	331.87	46.47	-1.58	2.92	0.27	-0.27	0.1031	829.90	35.60	0.79	791.73	-246.24	344.47		
800101	160000.	376.14	4.31	-1.07	-0.82	-1.87	-358.16	-0.3938	3045.76	349.40	-3.02	-3023.72	-108.08	1.41		
800101	180000.	300.53	-20.72	0.90	-1.12	1.18	-1.24	-1.0090	7758.30	427.55	-7.75	-7745.61	-118.39	7.71		
800101	200000.	268.32	30.87	2.16	0.01	-0.12	0.03	-1.3814	10605.06	67.12	-10.60	-10604.83	16.26	359.38		
800101	220000.	113.58	-25.71	1.97	3.08	-1.55	1.44	-1.6586	12739.52	287.15	-12.73	-12733.15	282.25	355.61		
800102	0.	275.56	-14.00	-0.05	2.42	0.65	-0.78	-2.0490	15738.25	391.59	-15.73	-15733.01	108.21	357.94		
800102	20000.	174.56	11.24	-0.86	-2.09	1.67	-1.82	-2.3653	18159.49	85.55	-18.16	-18158.63	154.23	9.53		
800102	40000.	74.89	13.16	-0.52	-3.00	-2.03	1.86	-2.5524	19592.75	-19.64	-19.59	-19592.72	-22.86	346.46		
800102	60000.	150.54	-21.82	-0.37	-1.95	-1.27	1.09	-2.7453	21083.82	327.99	-21.08	-21081.00	-105.67	359.53		
800102	80000.	-1.57	-45.45	-0.05	1.45	2.56	-2.76	-3.0155	23149.74	278.33	-23.15	-23148.05	-28.80	12.65		
800102	100000.	142.42	85.35	-0.52	2.75	0.94	-1.14	-3.0665	23545.54	-360.06	-23.54	-23542.26	-157.24	348.25		
800102	120000.	-38.63	16.98	-1.40	1.81	-3.91	3.71	-2.9293	22492.86	-91.48	-22.49	-22492.67	10.46	4.62		
800102	140000.	-4.51	-64.70	-1.30	1.48	-0.12	-0.08	-3.0666	23546.17	473.65	-23.54	-23540.81	166.61	3.15		
800102	160000.	-61.32	16.54	-0.83	-0.35	2.35	-2.54	-3.1158	23922.35	-121.59	-23.92	-23922.04	6.10	357.14		
800102	180000.	-110.15	28.16	1.02	0.06	-2.18	1.99	-2.8687	22025.45	-259.32	-22.02	-22023.66	109.29	2.72		
800102	200000.	-68.41	-5.10	2.43	1.49	-0.14	-0.03	-2.6386	20259.68	-3.32	-20.26	-20259.19	-141.42	354.53		
800102	220000.	-167.17	10.30	1.19	1.89	0.99	-1.14	-2.3659	18167.15	-230.43	-18.17	-18164.99	-159.35	6.65		
800103	0.	-114.23	36.11	-0.74	0.74	-1.60	1.47	-1.9904	15283.48	-350.93	-15.28	-15279.18	-92.45	355.39		
800103	20000.	-312.41	-26.13	-0.99	-1.73	-1.40	1.29	-1.6309	12523.54	-132.41	-12.52	-12522.60	-76.87	357.94		
800103	40000.	-202.76	-26.22	-0.25	-2.43	0.99	-1.07	-1.3481	10349.61	-34.61	-10.35	-10349.14	92.37	8.14		
800103	60000.	-333.42	41.72	0.24	-1.44	1.72	-1.77	-0.9065	6985.24	-587.53	-6.96	-6960.07	76.68	352.29		
800103	80000.	-359.05	18.86	0.10	-0.41	-3.44	3.42	-0.2492	1966.27	-453.53	-1.91	-1913.18	-16.52	5.82		
800103	100000.	-324.62	-78.69	0.00	1.11	0.09	-0.08	0.1867	1448.63	208.29	1.43	1433.56	6.91	357.00		
800103	120000.	-482.02	7.34	-1.20	2.77	4.04	-3.99	0.6277	4849.92	-508.58	4.82	4819.67	-183.93	355.90		
800103	140000.	-383.08	81.50	-1.69	-0.83	-1.19	1.29	1.4640	11277.53	-902.64	11.24	11239.63	-196.35	8.79		
800103	160000.	-483.05	-45.31	-0.05	-2.38	-2.53	2.67	2.1916	16826.88	-202.48	16.83	16825.45	-84.94	352.43		
800103	180000.	-502.62	-25.42	1.64	-2.15	1.96	-1.77	2.8421	21825.75	-311.47	21.82	21823.49	38.26	2.94		
800103	200000.	-592.34	30.79	2.46	-0.01	1.88	-1.63	3.7878	29089.01	-744.17	29.08	29078.04	290.13	2.13		
800103	220000.	-530.78	4.23	0.81	1.82	-1.59	1.89	4.8126	36954.96	-477.29	36.95	36951.80	77.16	356.58		
800104	0.	-545.68	-32.20	-0.58	-3.09	1.36	-0.98	5.6795	43605.44	-192.70	43.60	43604.75	152.50	2.74		

Table No. 2 -- Cowell Drag Versus Brouwer-Lyddane

DATE OF DATA		POSITION DIFFERENCES (METERS)			POSITION DIFFERENCES DEGREES				POSITION DIFFERENCES (METERS)			POSITION DIFFERENCES (METERS) (DEG.)		
YYMMDD	HHMMSS	DA	PPM DE	(10**+3) DI	DELH	DELG	DELM	DELTIME	TOTAL ERROR	RADIAL	IN TRACK	ALONG TRACK	CROSS TRACK	TRUE ANOMALLY
800101	0.	-42.47	62.17	0.35	2.03	-358.28	358.27	-0.1073	954.03	-466.68	-0.82	-824.03	-115.61	360.00
800101	20000.	66.62	16.37	-1.19	-0.25	-4.77	4.77	0.0799	642.93	-135.65	0.61	613.21	-137.60	350.43
800101	40000.	-118.56	-69.17	-0.61	-1.59	-0.22	0.21	-0.0216	389.17	-165.83	-0.17	-165.82	-29.60	1.24
800101	60000.	51.51	9.18	0.22	-1.57	4.16	-4.16	-0.1189	923.44	-126.79	-0.91	-912.82	58.43	13.49
800101	80000.	-89.44	42.92	0.11	0.13	-3.89	3.88	0.0184	499.63	-479.18	0.14	141.08	10.87	339.56
800101	100000.	-38.35	-48.08	0.10	0.97	357.28	-357.28	0.0902	752.99	289.41	0.69	692.99	54.86	1.60
800101	120000.	-7.36	-72.28	-0.27	2.78	3.27	-3.28	-0.1217	999.30	354.11	-0.93	-934.12	-25.10	19.13
800101	140000.	-68.59	62.26	-1.57	3.01	1.05	-1.06	-0.1309	1128.02	-447.29	-1.00	-1005.04	-249.53	344.47
800101	160000.	2.55	14.83	-1.05	-0.84	-2.44	-357.56	0.0026	146.23	-96.83	0.02	19.79	-107.77	1.41
800101	180000.	-51.13	-31.02	0.88	-1.31	0.63	-0.63	-0.0936	743.38	149.16	-0.72	-718.39	-119.49	7.71
800101	200000.	-55.72	26.83	2.16	-0.10	0.49	-0.49	-0.0145	262.78	-237.10	-0.11	-111.13	22.10	359.38
800101	220000.	-151.16	-20.50	2.03	2.68	-1.07	1.07	0.0831	696.32	-21.06	0.64	637.59	279.11	355.61
800102	0.	20.43	-7.68	-0.12	2.08	0.61	-0.61	0.0746	586.02	74.89	0.57	572.64	99.47	357.94
800102	20000.	-32.88	10.26	-0.77	-2.44	1.24	-1.23	0.0857	690.05	-126.49	0.66	657.81	165.72	9.53
800102	40000.	-97.39	-1.20	-0.56	-3.68	-0.94	0.95	0.0776	605.80	-107.66	0.60	595.88	-18.37	346.46
800102	60000.	7.59	-8.99	-0.39	-2.24	-0.35	0.36	0.0692	549.87	67.90	0.53	531.76	-122.39	359.53
800102	80000.	-104.01	-24.18	0.05	0.73	1.62	-1.61	0.0147	117.54	23.03	0.11	113.18	-21.78	12.65
800102	100000.	64.74	52.19	-0.64	2.20	0.67	-0.67	0.0025	303.85	-267.28	0.02	19.35	-143.22	348.25
800102	120000.	-61.07	12.10	-1.29	1.37	-1.94	1.94	0.0909	709.17	-125.79	0.70	697.89	-6.14	4.62
800102	140000.	-19.66	-25.66	-1.34	0.66	-0.25	0.25	0.0136	247.69	154.95	0.10	104.43	162.59	3.15
800102	160000.	-49.10	-2.82	-0.85	-0.69	0.59	-0.59	-0.0382	295.43	-26.36	-0.29	-293.16	25.36	357.14
800102	180000.	-29.96	-10.66	1.11	-0.62	0.30	-0.30	-0.0928	720.75	40.78	-0.71	-712.25	102.51	2.72
800102	200000.	13.21	41.95	2.33	0.98	1.54	-1.54	-0.0334	393.08	-255.27	-0.26	-256.60	-153.30	354.53
800102	220000.	-35.76	33.74	1.28	1.52	-1.74	1.74	0.1652	1299.38	-240.64	1.27	1268.57	-145.61	6.65
800103	0.	55.94	-30.70	-0.75	0.15	-0.84	0.85	0.1061	858.98	257.09	0.81	814.74	-89.15	355.39
800103	20000.	-115.94	-2.63	-1.01	-1.95	1.84	-1.83	0.0085	144.01	-92.77	0.07	65.00	-88.92	357.94
800103	40000.	28.90	40.77	-0.20	-2.79	-1.40	1.41	0.0945	766.54	-228.20	0.73	725.44	96.13	8.14
800103	60000.	-60.04	-29.71	0.22	-1.65	-0.82	0.83	0.0566	460.23	126.22	0.43	434.76	82.85	352.29
800103	80000.	-53.59	-17.44	0.12	-0.49	0.57	-0.57	-0.0213	173.73	55.90	-0.16	-163.35	-19.36	5.82
800103	100000.	5.78	11.21	0.01	1.12	0.14	-0.14	-0.0072	89.17	-69.49	-0.06	-55.58	5.74	357.00
800103	120000.	-124.11	-18.77	-1.18	2.81	-0.28	0.27	-0.0027	187.01	0.01	-0.02	-20.75	-185.86	355.90
800103	140000.	18.98	-13.34	-1.73	-0.52	1.44	-1.44	-0.1340	1049.67	84.16	-1.03	-1028.69	-191.13	8.79
800103	160000.	-37.35	44.10	0.05	-1.97	1.08	-1.09	-0.1558	1240.43	-320.32	-1.20	-1195.81	-78.09	352.43
800103	180000.	-53.15	21.69	1.56	-1.81	356.96	-356.96	0.0241	266.36	-189.68	0.19	185.40	24.35	2.94
800103	200000.	-76.11	-83.95	2.50	0.99	0.05	-0.05	-0.0561	715.62	491.93	-0.43	-430.82	290.71	2.13
800103	220000.	19.77	32.17	0.91	2.34	-355.94	355.94	-0.1480	1155.90	-184.94	-1.14	-1136.43	102.10	356.58
800104	0.	-7.22	76.00	-0.78	-1.87	-2.69	2.70	0.0979	921.52	-515.32	0.75	751.99	134.73	2.74

Table No. 3 -- Cowell Drag Versus Bg

Table # 4

## SMM IN TRACK ERROR (km.)

		COWELL	• Bg		COWELL	• Bg		COWELL	• Bg	
	EPOCH	80/03/14	80/03/14		80/03/20	80/03/20		80/08/0/	80/08/0/	
0	L.C.	-0.02	-0.32		0.13	0.06		0.09	0.21	
2	ARC	-0.05	0.22		-0.18	-0.04		0.12	0.85	
	PREDICTS									
2	"	-0.44	0.66		-2.96	-1.87		2.41	2.31	
4	"	-2.82	-0.81		-6.78	-4.08		6.43	4.67	
6	"	-10.39	-7.46		-19.62	-14.66		13.02	8.73	
8	"	-27.15	-23.28		-42.60	-34.60		22.88	15.28	
10	"	-51.66	-46.88		-77.20	-65.26		38.18	26.60	
12	"	-91.94	-86.26		-123.75	-106.96		62.09	45.88	
14	"	-149.09	-142.39		-176.93	-154.47		95.58	74.00	
16	"	-224.58	-216.62		-237.02	-208.23		141.93	114.11	

## REFERENCES

1. Brouwer, D., "Solution of the Problem of Artificial Satellite Theory Without Drag," The Astronomical Journal, Volume 64, October, 1959, pages 378-397.
2. Von Zeipel, H., Arkiv Mathematics, Astronomy, Physics, Volume 11, No. 1, 1916.
3. Lyddane, R. H., "Small Eccentricities or Inclinations in the Brouwer Theory of Artificial Satellite Motion," The Astronomical Journal, Volume 68, June, 1963, pages 555-558.
4. Gordon, R. A., Mistretta, G. D., and Watson, J. S., "A Comparison of Classical Analytic Theories for the Motion of Artificial Satellites," Journal of Guidance and Control, Volumes 2 and 3, May and June, 1979, page 184.
5. Walter, H. G., "Conversion of Osculating Orbital Elements into Mean Elements," The Astronomical Journal, Volume 72, October 1967, pages 994-997.

## Appendix

$$\underline{\Omega}(t) = \underline{B}_g(\underline{\bar{\Omega}}(t_0), t)$$

Geodynamic Constants:

$$Gm = 398600.8 \text{ km}^3/\text{sec}^2$$

$$a_e = 6378.14 \text{ km}$$

$$\mu = 1$$

$$R_e = 1$$

$$k_e = \sqrt{\frac{Gm}{a_e^3}}$$

Zonal Harmonics:

$$J_2 = -0.0010826517$$

$$J_3 = 0.0000025450306$$

$$J_4 = 0.0000016714987$$

$$k_2 = -\frac{1}{2} J_2 R_e^2$$

$$k_3 = J_3 R_e^3$$

$$k_4 = J_4 R_e^4$$

Define fractions:

$$\frac{1}{2}, \frac{1}{3}, \frac{1}{4}, \frac{3}{2}, \frac{3}{8}, \frac{3}{32}, \frac{5}{4}, \frac{5}{16}, \frac{15}{16}$$

Input:  $\underline{B}_{RWGOR}(\underline{\bar{\Omega}}, \underline{\Omega}, \text{IDPERT}, \text{IDPASS}, \text{IDMEAN}, \underline{\beta}, t)$

$$\underline{\bar{\Omega}}(t_0) = (a_0'', e_0'', i_0'', h_0'', g_0'', l_0'') \text{ epoch mean elements.}$$

$a$  = Semi-major axis

$e$  = eccentricity

$i$  = inclination

$g$  = argument of perigee

$h$  = Longitude of ascending node

$l$  = Mean anomaly

$$\text{IDPERT} = \begin{cases} 1 \rightarrow \underline{B}_g(\underline{\bar{\Omega}}(t_0), t) \text{ evaluate secular elements} \\ \neq 1 \rightarrow \underline{B}_g(\underline{\Omega}(t), t) \text{ evaluate osculating elements} \end{cases}$$

$$\text{IDPASS} = \begin{cases} 1 \rightarrow \underline{B}_g(\underline{\bar{\Omega}}(t_0), t) \text{ initialize theory at } t=0 \text{ epoch} \\ 2 \rightarrow \underline{B}_g(\underline{\Omega}(t), t) \text{ evaluate theory at time } (t) \end{cases}$$

$$IDMEAN = \begin{cases} 0 \rightarrow B_g(t=0, \underline{\Omega}) & \text{osculating elements input} \\ & \text{for osculating to mean conversion} \\ \neq 0 \rightarrow B_g(t, \underline{\Omega}) & \text{Mean elements input} \\ & \text{for updating osculating elements} \end{cases}$$

Output:

$$\underline{\Omega}_i'' = (a'', e'', i'', h'', g'', l'')$$

$$\underline{\Omega}_i = (a, e, i, h, g, l)$$

$$B_i = (E', P, g', n, f')$$

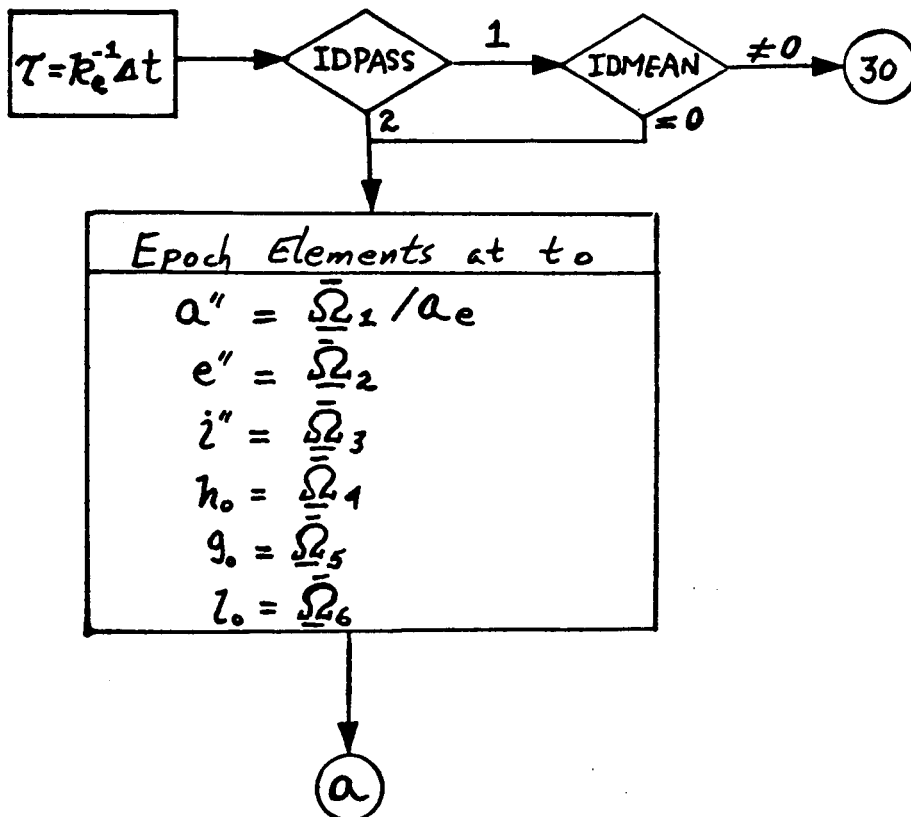
$E'$  -- Long Period Eccentric Anomaly

$P$  -- mean Period

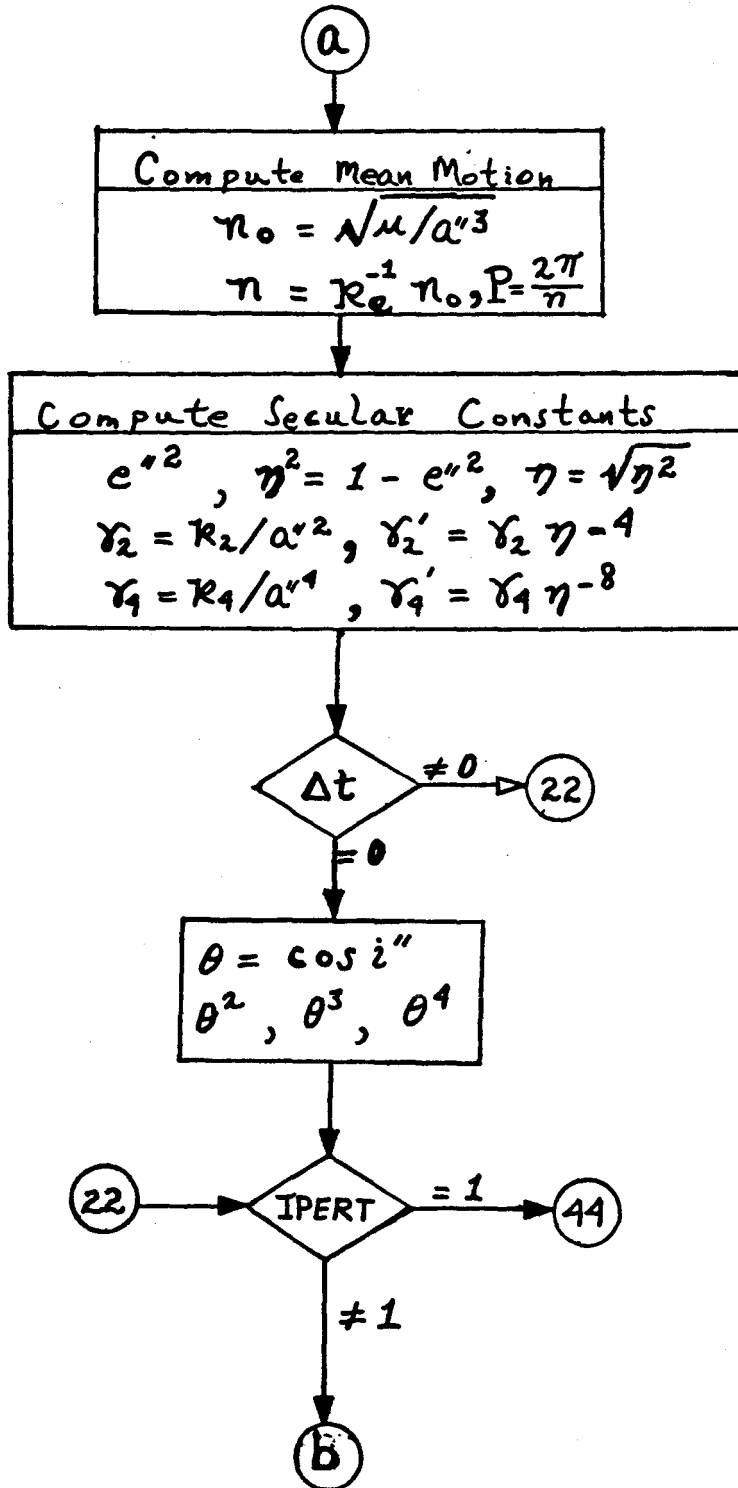
$g'$  -- Long Period argument of perigee

$n$  -- "mean" mean motion

$f'$  -- Long Period true anomaly







(b)

Compute Short-Period constants  
Compute Long-Period constants

$$\eta^3, \eta^6, \gamma_3 = \kappa_3 / a''^3, \gamma_3' = \gamma_3 \eta^{-6}$$

$$\gamma_3' / \gamma_2'$$

Δt ≠ 0 → (33)

Δt = 0

$\sin i'', \tan i'', 3\theta^2 - 1, 1 - \theta^2$   
 $\sqrt{1 - \theta^2}, 3(1 - \theta^2)$   
 $A_0 = \theta^2 / (1 - 5\theta^2)$   
 $A_1 = 1/8 (1 - 11\theta^2 - 40\theta^2 A_0)$   
 $A_3 = -1/8 \theta (11 + 80A_0 + 200A_0^2)$

(33)

$3e'', 1/2 \gamma_2', 1/2 \gamma_2' \theta,$   
 $1/2 \gamma_2' \theta^2 \sqrt{1 - \theta^2}$

(c)

(C)

$$A_2 = \eta^3 \gamma_2' A_1 - \frac{1}{16} \gamma_2' \left\{ \begin{array}{l} 2 + e^{\eta^2} - 400e^{\eta^2} \theta^2 A_0^2 \\ -40(5e^{\eta^2} + 2)\theta^2 A_0 \\ -11\theta^2(3e^{\eta^2} + 2) \end{array} \right\}$$

$$A_4 = \frac{1}{4} (\gamma_3' / \gamma_2') \text{Sin } i'' \quad , \quad A_5 = e^{\eta} \theta A_4 / (1 + \theta)$$

(44) → IDMEAN = 0 → (50)

≠ 0

(30) → IDPASS = 2 → (40)

≠ 2

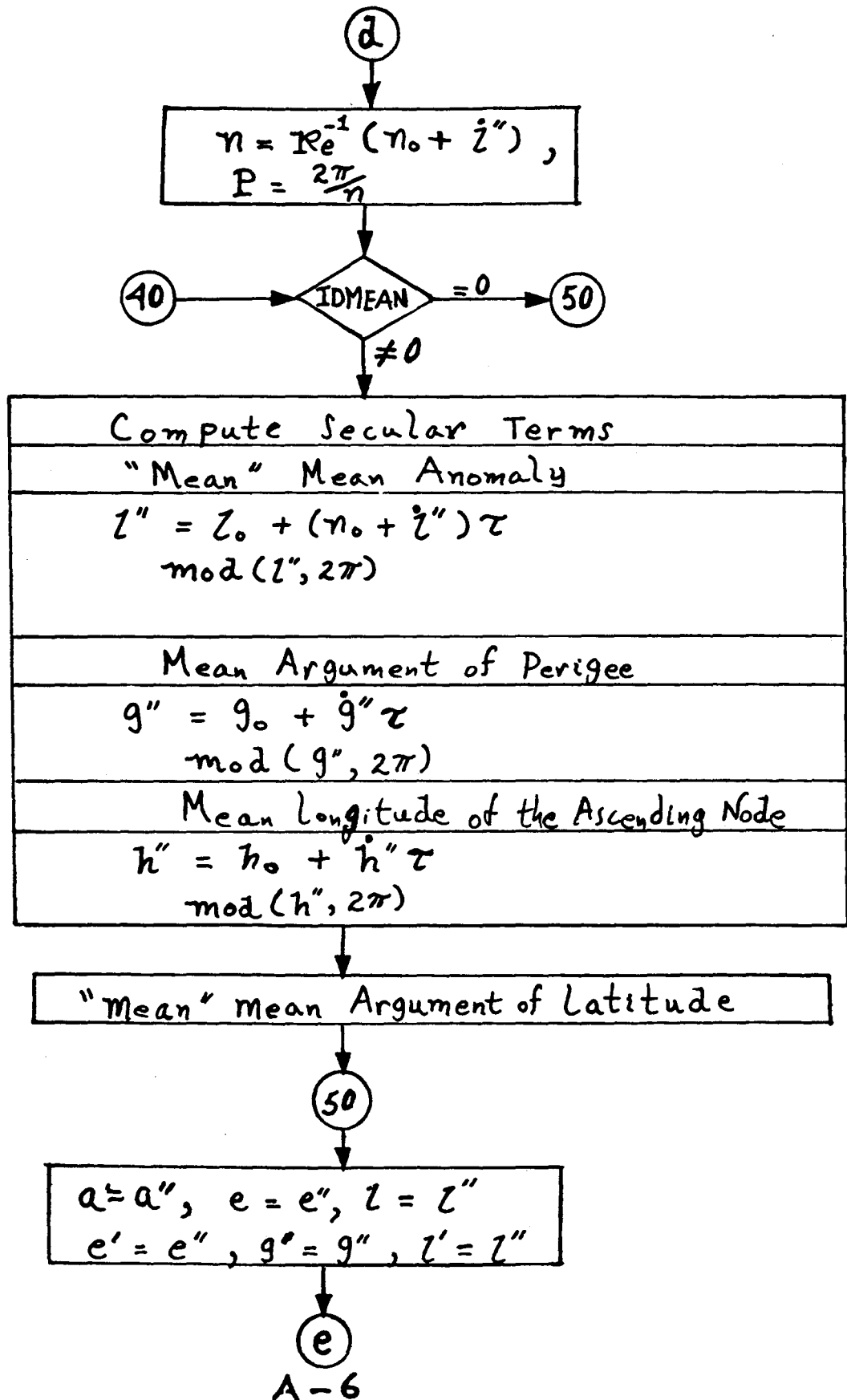
Compute  $\dot{z}''$ ,  $\dot{q}''$ ,  $\dot{h}''$

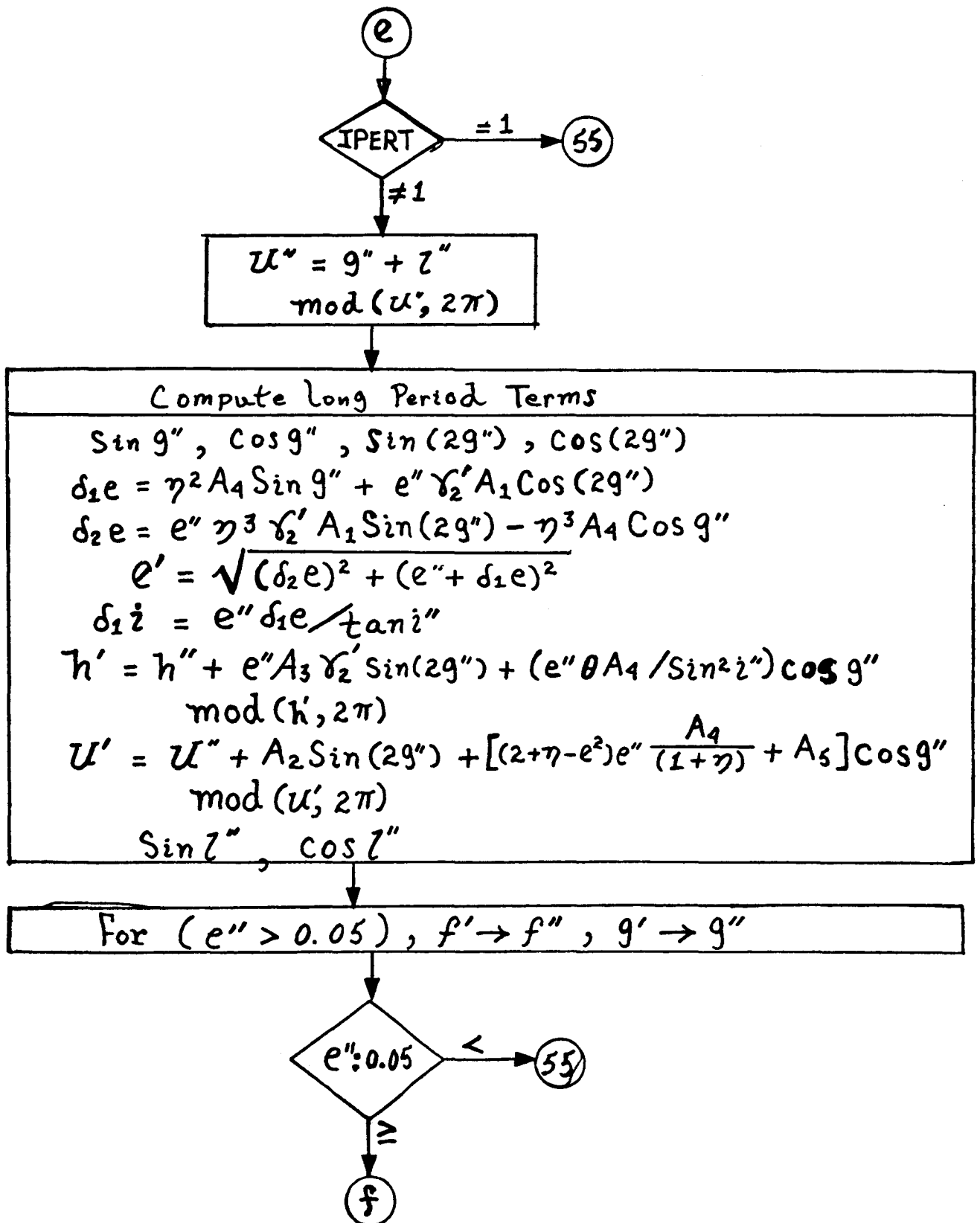
$$\dot{z}'' = \left\{ \begin{array}{l} \gamma_2' \left[ \frac{3}{2} (3\theta^2 - 1) + \gamma_2' \left( \frac{3}{32} \right) [\theta^2 (30 - 96\eta - 90\eta^2) \right. \right. \\ \left. \left. + (16\eta + 25\eta^2 - 15) + \theta^4 (144\eta + 25\eta^2 + 105)] \right] \right\} \eta \eta_0 \\ + e^{\eta^2} \gamma_4' \left( \frac{15}{16} \right) (3 + 35\theta^4 - 30\theta^2) \end{array} \right.$$

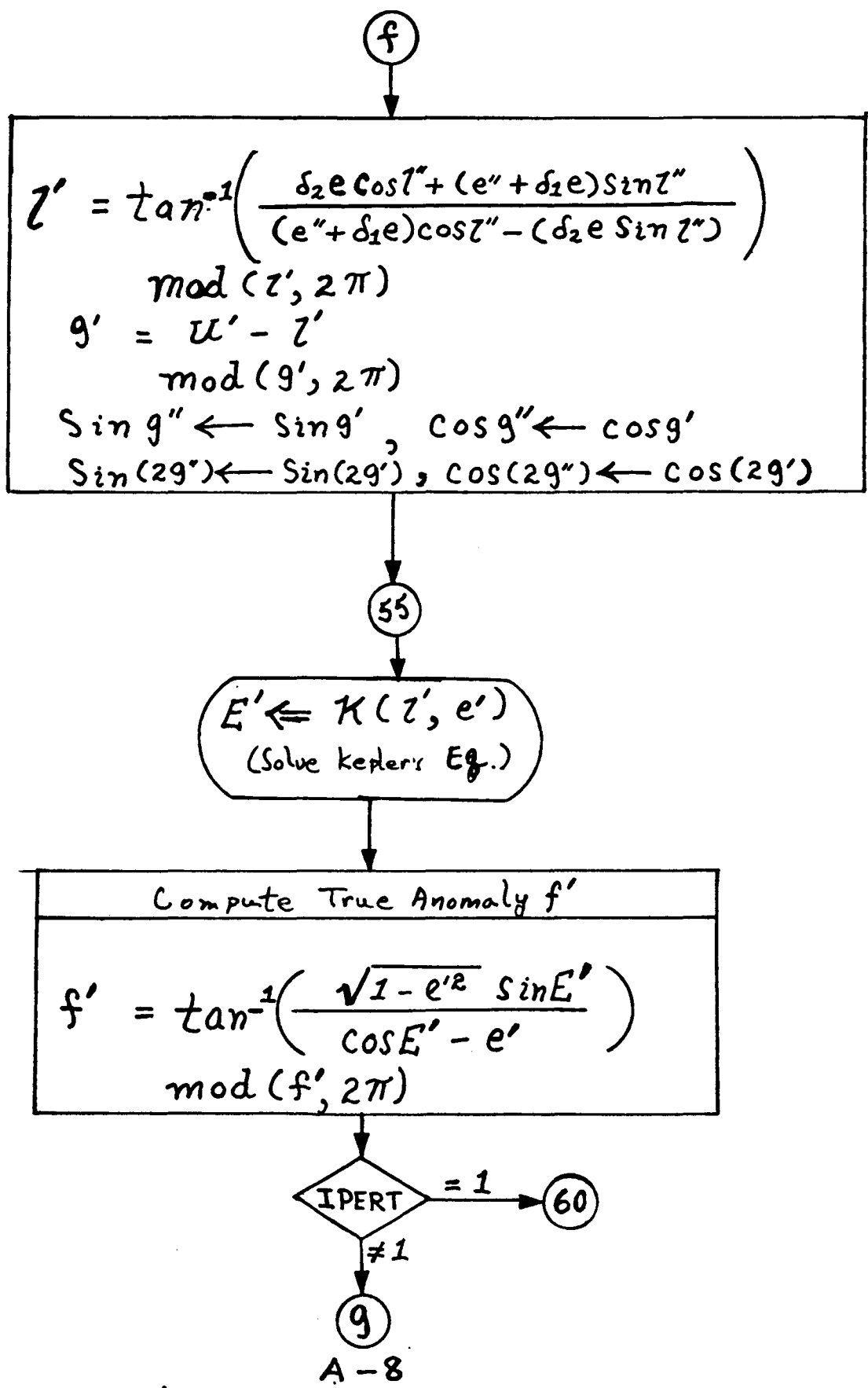
$$\dot{q}'' = \eta_0 \left\{ \begin{array}{l} \frac{3}{2} \gamma_2' (5\theta^2 - 1) + \frac{3}{32} \gamma_2'^2 [25\eta^2 + 24\eta - 35 \\ + (90 - 192\eta - 126\eta^2)\theta^2 + (385 + 360\eta + 45\eta^2)\theta^4] \\ + \frac{5}{16} \gamma_4' [21 - 9\eta^2 + (126\eta^2 - 270)\theta^2 + (385 - 189\eta^2)\theta^4] \end{array} \right.$$

$$\dot{h}'' = \eta_0 \left\{ \begin{array}{l} -3\gamma_2' \theta \\ \frac{3}{8} \gamma_2'^2 [(9\eta^2 + 12\eta - 5) + (-5\eta^2 - 36\eta - 35)\theta^3] \\ \frac{5}{4} \gamma_4' (5 - 3\eta^2) \theta (3 - 7\theta^2) \end{array} \right.$$

(D)







9

$$\alpha = \frac{1}{1 - e' \cos E'}$$

$$\alpha^2, \alpha^3$$

$$\sin f' = d \sqrt{1 - e'^2} \sin E'$$

$$\cos f' = \alpha (\cos E' - e')$$

$$\cos^2 f', \cos(2f'), \sin(2f'), \cos(3f'), \sin(3f')$$

$$\sin(2g' + f'), \sin(2g' + 2f'), \sin(2g' + 3f')$$

$$\cos(2g' + f'), \sin(2g' + 2f'), \sin(2g' + 3f')$$

Semi - major Axis

$$a = a'' \left\{ 1 + \frac{1}{2} \left[ (3\theta^2 - 1)(\alpha^3 - \eta^{-3}) + 3(1 - \theta^2)\alpha^3 \cos(2g' + 2f') \right] \right\}$$

h

(B<sub>9</sub>)

(h)

Compute eccentricity

$$\delta_1 e = \delta_1 e + \frac{1}{2} \eta^2 \left\{ \begin{array}{l} 3 \left( \frac{1}{\eta^6} \right) \gamma_2 (1 - \theta^2) \cos(2g' + 2f') [3e'' \cos^2 f' + 3 \cos f' + e''^2 \cos^3 f' + e''] \\ - \gamma_2' (1 - \theta^2) [3 \cos(2g' + 2f') + \cos(3f' + 2g')] \\ (3\theta^2 - 1) \gamma_2 \left( \frac{1}{\eta^6} \right) [e'' \eta + \left( \frac{e''}{1 + \eta} \right) + 3e'' \cos^2 f' + 3 \cos f' + e''^2 \cos^3 f'] \end{array} \right\}$$

$$\delta_2 e = \delta_2 e - \frac{1}{4} \eta^3 \gamma_2' \left\{ \begin{array}{l} 2(3\theta^2 - 1)(d^2 \eta^2 + \alpha + 1) \sin f' \\ + 3(1 - \theta^2) \left[ \begin{array}{l} (-d^2 \eta^2 - \alpha + 1) \sin(2g' + f') \\ + (d^2 \eta^2 + \alpha + \frac{1}{3}) \sin(3g' + f') \end{array} \right] \end{array} \right\}$$

$$e = \sqrt{(\delta_2 e)^2 + (e'' + \delta_1 e)^2}$$

compute i inclination

$$\dot{i} = \dot{i}'' + \delta_1 \dot{i} + \frac{1}{2} \gamma_2' \theta \sqrt{1 - \theta^2} [3 \cos(2g' + 2f') + 3e'' \cos(2g' + f') + e'' \cos(2g' + 3f')] \text{ mod}(i, 2\pi)$$

compute h longitude of the ascending node

$$h = h' - \frac{1}{2} \gamma_2' \theta [6(f' - l' + e'' \sin f') - 3 \sin(2g' + 2f') - 3e'' \sin(2g' + f') - e'' \sin(2g' + 3f')] \text{ mod}(h, 2\pi)$$

(i)



i

compute (U) - Mean Argument of Latitude

$$U = U' + \left(\frac{1}{\eta+1}\right) \frac{1}{4} e'' \gamma_2' \eta^2 \left\{ \begin{array}{l} 3(1-\theta^2) \left[ \begin{array}{l} (\frac{1}{3} + \alpha^2 \eta^2 + \alpha) \sin(3f' + 2g') \\ (1 - \eta^2 \alpha^2 - \alpha) \sin(2g' + f') \end{array} \right] \\ + 2(3\theta^2 - 1)(\eta^2 \alpha^2 + \alpha + 1) \sin f' \end{array} \right\}$$

$$+ \frac{3}{2} \gamma_2' (5\theta^2 - 1)(e'' \sin f' + f' - l')$$

$$+ \frac{1}{4} \gamma_2' (3 - 5\theta^2) \left\{ \begin{array}{l} e'' \sin(2g' + 3f') \\ 3[\sin(2g' + 2f') + e'' \sin(2g' + f')] \end{array} \right\}$$

$\text{mod}(U, 2\pi)$

compute l mean Anomaly

$$l = \tan^{-1} \left( \frac{\delta_2 e \cos l'' + (e'' + \delta_1 e) \sin l''}{(e'' + \delta_1 e) \cos l'' - (\delta_2 e \sin l'')} \right)$$

$\text{mod}(l, 2\pi)$

j

$(B_g)$  $(j)$ 

Compute  $g$  Argument of Perigee

$$g = u - \tau$$
$$\text{mod } (g, 2\pi)$$

Store Secular, osculating arrays

$$a'' = a' a_e$$
$$a = a a_e$$

$\bar{\Omega}, \underline{\Omega}, B$

END